Journal of Nuclear Materials 407 (2010) 44–47

Contents lists available at ScienceDirect

Journal of Nuclear Materials

journal homepage: www.elsevier.com/locate/jnucmat

Microstructural evolution in irradiated uranium-bearing delta-phase oxides $A_6U_1O_{12}$ (A = Y, Gd, Ho, Yb, and Lu)

M. Tang [a,*], K.S. Holliday [b], J.A. Valdez [a], B.P. Uberuaga [a], P.O. Dickerson [a], R.M. Dickerson [a], Y. Wang [a], K.R. Czerwinski [b], K.E. Sickafus [a]

[a] *Materials Science & Technology Division, Mail Stop G755, Los Alamos National Laboratory, Los Alamos, NM 87545, USA*
[b] *Radiochemistry Group, University of Nevada, Las Vegas, NV 89154, USA*

ABSTRACT

Irradiation-induced microstructural evolution in uranium-bearing delta-phase oxides of $A_6U_1O_{12}$ (A = rare earth cations) were characterized using grazing incidence X-ray diffraction and transmission electron microscopy. Polycrystalline $Y_6U_1O_{12}$, $Gd_6U_1O_{12}$, $Ho_6U_1O_{12}$, $Yb_6U_1O_{12}$, and $Lu_6U_1O_{12}$ samples were irradiated with 300 keV Kr^{++} to a fluence of 2×10^{20} ions/m^2 at cryogenic temperature (~100 K). The crystal structure of these compounds was determined to be an ordered, fluorite derivative structure, known as the delta-phase, a rhombohedral symmetry belonging to space group $R\bar{3}$. Experimental results indicate that all these compounds are resistant to amorphization to a displacement damage dose of ~60 displacements per atom. In these experiments, we sometimes observed an irradiation-induced order-to-disorder phase transformation, from an ordered rhombohedral to a disordered fluorite structure.

1. Introduction

Actinide oxides have been used as nuclear fuel since the first controlled chain reaction in 1942. UO_2 and mixed oxides (MOX) which crystallize in the fluorite structure exhibit exceptional resistance to irradiation damage and are therefore still the predominant fuel for thermal power reactors. Compounds with structures similar to fluorite, have been proposed as potential materials for nuclear fuel forms [1,2] and nuclear waste immobilization [3]. Here, we investigate the ion irradiation damage properties of uranium-bearing oxides of the formula $A_6U_1O_{12}$ (A = rare earth cations) which is a fluorite structural derivative, and possesses rhombohedral symmetry with space group $R\bar{3}$, namely, the so-called delta (δ) phase [4,5]. These oxides are potential hosts for the immobilization of surplus actinides. They could be used as fuel forms for transmutation of actinides or waste forms for actinide disposal.

We showed recently [6] that δ-$Y_6U_1O_{12}$ is very resistant to amorphization under 300 keV Kr^{++} irradiation at cryogenic temperature, but undergoes a partially order-to-disorder (O–D) phase transformation, from an ordered rhombohedral to a disordered fluorite phase, at a relatively high displacement damage dose 50 displacements per atom (dpa). The present study is an extension of our earlier work and in this paper we report a comparative study of crystal structural evolution in $Y_6U_1O_{12}$, $Gd_6U_1O_{12}$, $Ho_6U_1O_{12}$, $Yb_6U_1O_{12}$, and $Lu_6U_1O_{12}$ samples, all of which possess the delta-phase prior to irradiation. We observed here that Kr irradiation induces a complete O–D phase transformation in $Gd_6U_1O_{12}$ and $Yb_6U_1O_{12}$; while there is no fully O–D phase transformation in the irradiated $Y_6U_1O_{12}$, $Ho_6U_1O_{12}$, and $Lu_6U_1O_{12}$ samples.

2. Experimental

High purity Y_2O_3, Gd_2O_3, Ho_2O_3, Yb_2O_3, Lu_2O_3 powders from Alpha Aesar (99.9%–99.99% purity), were mixed with UO_2 powder from Bio-Analytical Industries, in the molar ratio of 1:3, then ball milled in a stainless steel cup and pressed to a pressure of 6 tons in a SPEX 13 mm die. These pressed pellets were oxidized in a box furnace for 12 h at 1000 °C under air, then remilled, repressed and resintered in air at 1500 °C for 48 h in a Mellen high temperature tube furnace. X-ray diffraction measurements on these samples showed that the sintered pellets consisted pure δ-phase $A_6U_1O_{12}$. The pellets were cut into 0.5 mm thickness discs using a diamond saw and then polished with alumina lapping films to obtain a mirror finish. Ion irradiation was performed at cryogenic temperature (~100 K) in the Ion Beam Materials Laboratory at Los Alamos National Laboratory, using a Danfysik high current ion implanter operating at 150 kV. 300 keV Kr^{++} ions were implanted at normal incidence using a dose rate of 1×10^{16} Kr/m^2 s to a fluence of 2×10^{20} Kr/m^2. Irradiated samples were analyzed using both grazing incidence X-ray diffraction (GIXRD) and transmission electron microscopy (TEM). GIXRD measurements were performed using a Bruker AXS D8 advanced X-ray diffractometer at a gracing incidence angle of $\alpha = 0.35°$, which we estimate to be close to the critical angles $\alpha_c = 0.35°–0.45°$ for these delta-phase

---

[*] Corresponding author. Tel.: +1 505 665 1472; fax: +1 505 667 8021.
E-mail address: mtang@lanl.gov (M. Tang).

0022-3115/$ - see front matter © 2010 Elsevier B.V. All rights reserved.
doi:10.1016/j.jnucmat.2010.07.007

compounds, based on the critical angle formula from Ref. [7]. Under these conditions, X-rays are scattered from the near surface of these samples within a depth usually less than 80 nm [8,9], i.e., significantly shallower than the range of the Kr ions (∼200 nm) into these materials. Thus, we believe that these measurements are sampling only the irradiated volume near the sample surface. Irradiated samples were prepared in cross-sectional geometry for TEM examination using a focused-ion-beam (FIB) apparatus, based on the in situ lift out method. TEM investigations were performed using a Philips CM-30 instrument operating at 300 kV.

3. Results and discussion

Fig. 1 shows GIXRD patterns obtained from $Gd_6U_1O_{12}$, $Yb_6U_1O_{12}$, $Y_6U_1O_{12}$, $Ho_6U_1O_{12}$, and $Lu_6U_1O_{12}$ samples (Fig. 1a–e, respectively), before and after 300 keV Kr^{++} ion irradiation to a fluence of 2×10^{20} Kr/m^2. This ion fluence corresponds to peak displacement damage doses of 50–65 dpa for these compounds (these are estimates based on the Monte Carlo ion transport code SRIM [10]; 40 eV was used for the displacement threshold energy for all target atoms in these calculations). The patterns obtained from pristine $Gd_6U_1O_{12}$, $Yb_6U_1O_{12}$, $Y_6U_1O_{12}$, $Ho_6U_1O_{12}$, and $Lu_6U_1O_{12}$ samples

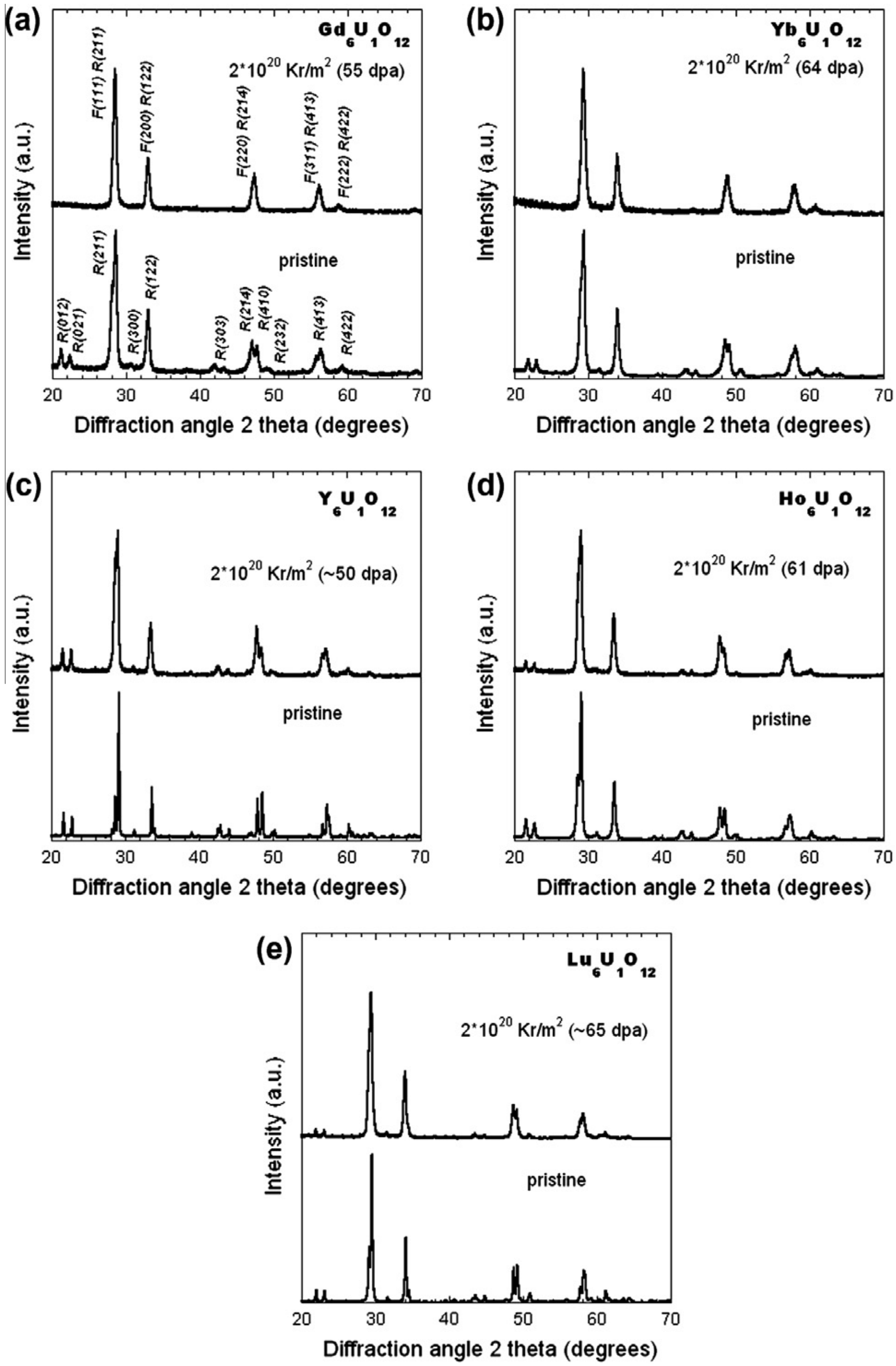

Fig. 1. Grazing incidence X-ray diffraction (GIXRD) patterns obtained from: (a) $Gd_6U_1O_{12}$, (b) $Yb_6U_1O_{12}$, (c) $Y_6U_1O_{12}$, (d) $Ho_6U_1O_{12}$, (e) $Lu_6U_1O_{12}$, before and after irradiation with 300 keV Kr^{++} ions at 100 K. The angle of incidence of the X-rays for these measurements was $\alpha = 0.35°$.

show primarily diffractions of representative of the rhombohedral δ-phase structure (diffraction peaks labeled '*R*') [11]. This indicates that the pristine crystal structures of these samples possess delta-phase structure (space group $R\bar{3}$). Comparison of the GIXRD patterns in Fig. 1a–e reveals significant differences in the irradiation response of these compounds. For irradiated $Gd_6U_1O_{12}$ and $Yb_6U_1O_{12}$, some XRD diffractions are almost absent; while the GIXRD patterns do not show any new features except for the diminish of some diffraction peaks in irradiated $Y_6U_1O_{12}$, $Ho_6U_1O_{12}$, and $Lu_6U_1O_{12}$. We describe these differences next.

3.1. $Gd_6U_1O_{12}$, and $Yb_6U_1O_{12}$

The GIXRD patterns in Fig. 1a and b indicate that "superlattice" diffractions, such as *R(0 1 2)*, *R(0 2 1)*, *R(3 0 0)*, *R(3 0 3)*, *R(4 1 0)*, and *R(2 3 2)* (marked on the graph), disappear almost entirely by the fluence of 2×10^{20} Kr/m^2. On the other hand, the principal diffraction maxima, which index as *R(2 1 1)*, *R(1 2 2)*, *R(2 1 4)*, *R(4 1 3)*, and *R(4 2 2)*, are more or less unaffected by irradiation. The *δ-phase R(2 1 1)*, *R(1 2 2)*, *R(2 1 4)*, *R(4 1 3)*, and *R(4 2 2)* diffractions are identified with the "parent" cubic fluorite (*F*) structure (corresponding to *F(1 1 1)*, *F(2 0 0)*, *F(2 2 0)*, *F(3 1 1)*, and *F(2 2 2)* diffractions). These observations suggest that Kr^{++} ion irradiation induces a complete phase transformation from an ordered δ-phase to a structure indistinguishable from a cubic fluorite phase.

3.2. $Y_6U_1O_{12}$, $Ho_6U_1O_{12}$, and $Lu_6U_1O_{12}$

The GIXRD patterns in Fig. 1c, d and e indicate almost all delta-phase diffraction peaks still exist, although the weakest δ-phase peaks decrease in intensity more than the five most prominent diffraction peaks. These observations suggest that these materials are gradually undergoing an O–D transformation from an ordered δ-phase structure to a disordered fluorite structure, but not completely transformed.

It is also noteworthy that, despite some of these compounds experience a complete O–D phase transformation, no amorphization was observed in all these δ-phase $A_6U_1O_{12}$ compounds in this displacive irradiation environment, up to a maximum ion dose of 65 dpa.

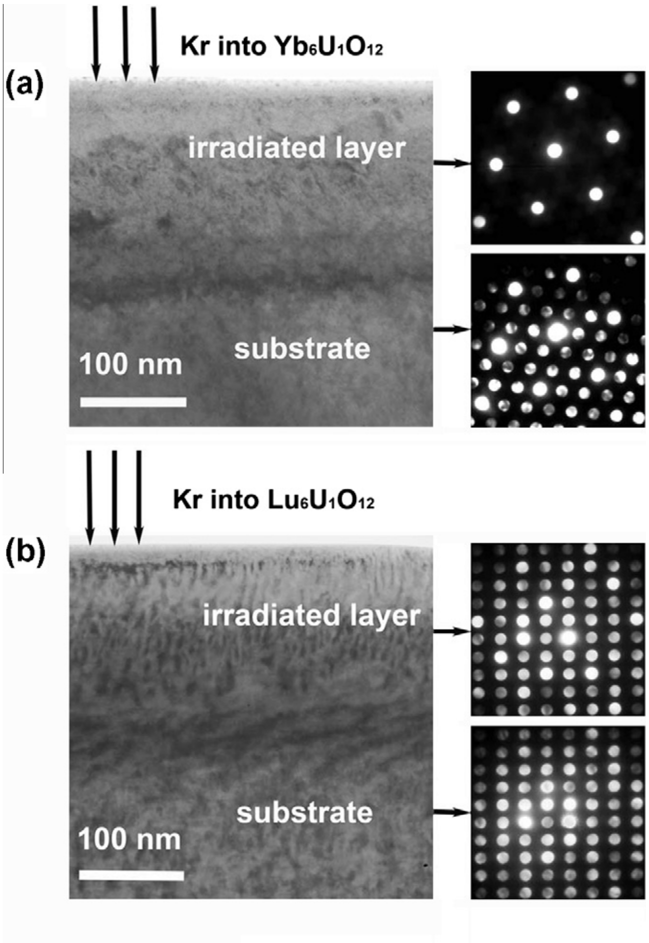

Fig. 2. Cross-sectional TEM bright-field image and microdiffraction (μD) patterns obtained from: (a) $Yb_6U_1O_{12}$ and (b) $Lu_6U_1O_{12}$. Samples were irradiated to a fluence of 2×10^{20} Kr/m^2 at 100 K. The disappearance of specific diffraction spots (top μD patterns) suggests that there is a fully O–D phase transformation in the irradiated $Yb_6U_1O_{12}$. No fully O–D phase transformation was observed in the irradiated $Lu_6U_1O_{12}$.

Fig. 2 shows cross-sectional TEM observations of 300 keV Kr^{++} ion irradiated $Yb_6U_1O_{12}$ and $Lu_6U_1O_{12}$ samples (Fig. 2a and b respectively), at a fluence of 2×10^{20} Kr/m^2. The micrographs reveal that the irradiated layers in $Yb_6U_1O_{12}$ and $Lu_6U_1O_{12}$ have a similar thickness of around 200 nm. In Fig. 2a, the microdiffraction (μD) patterns indicate no diffuse halo (which would be expected from an amorphous structure), but a change in structure is apparent between the unirradiated substrate (bottom μD pattern) and the irradiated layer (top μD patterns). The μD pattern obtained from the irradiated region in Fig. 2a is consistent with a single phase, cubic fluorite structure, oriented with an epitaxial relationship with the unirradiated substrate (beam direction $\overrightarrow{B} = [1\,1\,1]_F$. in the irradiated region; $\overrightarrow{B} = [0\,0\,1]_R$ in the substrate). The substrate μD pattern is consistent with the rhombohedral δ-phase $Yb_6U_1O_{12}$ structure (using the 3-index system for indexing hexagonal directions). Superlattice reflections associated with the rhombohedral δ-phase are seen to completely disappear in the top μD patterns obtained from different irradiated areas. These TEM observations indicate that the O–D transformation of $Yb_6U_1O_{12}$ is fully complete by the Kr^{++} ion dose of ~64 dpa. Similar microstructural evolution was observed in irradiated $Gd_6U_1O_{12}$ (data not shown here). In Fig. 2b, the μD patterns (beam direction $\overrightarrow{B} = [0\,1\,3]_R$) indicate there is no apparent change in structure between the unirradiated substrate (bottom μD pattern) and the irradiated layer (top μD patterns). These TEM observations show that there is no fully O–D transformation in irradiated $Lu_6U_1O_{12}$ at the Kr ion dose of 65 dpa. Similar results were observed in ion irradiated $Ho_6U_1O_{12}$ and $Y_6U_1O_{12}$ (data not shown here). TEM results in Fig. 2 are consistent with the GIXRD results shown in Fig. 1.

GIXRD and TEM observations indicate different microstructural changes in irradiated $Y_6U_1O_{12}$, $Gd_6U_1O_{12}$, $Ho_6U_1O_{12}$, $Yb_6U_1O_{12}$, and $Lu_6U_1O_{12}$, including a fully O–D phase transformation in $Gd_6U_1O_{12}$ and $Yb_6U_1O_{12}$, and no fully O–D transformation in $Y_6U_1O_{12}$, $Ho_6U_1O_{12}$, and $Lu_6U_1O_{12}$. Our observation of O–D phase transformation in these irradiated δ-phase compounds is attributable to the formation of cation antisites and anion vacancies randomly distributed over all sites. Under a displacive irradiation environment, an elevated population of point defects (such as cation antisite defects form on the cation sublattice and anion Frenkel defects on the anion sublattice) is produced in these δ-phase compounds. The accumulation of point defects often leads to defect clustering (such as formation of dislocation loops and voids), as well as to lattice instability which can result in phase transformation of the crystal. As a result of cation antisite and anion Frenkel defect formation and accumulation in δ-phase compounds, the rhombohedral symmetry of the ordered δ-phase evolve in favor of cubic symmetry which we refer as a disordered fluorite phase. The irradiation-induced O–D transformation from an ordered, δ-phase structure with rhombohedral symmetry to a disordered fluorite phase is analogous to that seen in previous radiation damage studies on 4:3:12 δ-phase compounds [12–14] and $A_2B_2O_7$ pyrochlore compounds [15–17].

A number of observations in this study are not explainable at this time. For instance, these uranium-bearing δ-phase compounds experience the different O–D transformation tendencies under 300 keV Kr^{++} irradiation. Work is in progress to resolve some of these seemingly intractable issues.

4. Summary

300 Kr^{++} irradiation experiment under cryogenic condition on polycrystalline δ-phase $Y_6U_1O_{12}$, $Gd_6U_1O_{12}$, $Ho_6U_1O_{12}$, $Yb_6U_1O_{12}$, and $Lu_6U_1O_{12}$ was performed. Irradiation-induced microstructural evolutions in these compounds were characterized by GIXRD measurement and TEM observation. A fully O–D phase transformation was observed in irradiated $Gd_6U_1O_{12}$ and $Yb_6U_1O_{12}$; while no fully O–D phase transformation in $Y_6U_1O_{12}$, $Ho_6U_1O_{12}$, and $Lu_6U_1O_{12}$. Our study indicates that these uranium-bearing δ-phase compounds exhibit significant amorphization resistance in a displacive irradiation environment, and could be used as fuel forms for transmutation of actinides or waste forms for actinide disposal.

Acknowledgements

This work was sponsored by the Seaborg Institute for Transactinium Science, Los Alamos National Laboratory, and the US Department of Energy, Office of Basic Energy Sciences, Division of Materials Sciences and Engineering.

References

[1] C. Degueldre, M. Pouchon, M. Doebeli, K.E. Sickafus, K. Hojou, G. Ledergerber, S. Abolhassani-Dadras, J. Nucl. Mater. 289 (2001) 115.
[2] C. Degueldre, J.-M. Paratte, Nucl. Technol. 123 (1998) 21.
[3] W.J. Weber, R.C. Ewing, C.R.A. Catlow, T. Diaz de la Rubia, L.W. Hobbs, C. Kinoshita, H. Matzke, A.T. Motta, M. Nastasi, E.K.H. Salje, E.R. Vance, S.J. Zinkle, J. Mater. Res. 13 (6) (1998) 1434.
[4] E.A. Aitken, S.F. Bartram, E.F. Juenke, Inorg. Chem. 3 (1964) 949.
[5] S.F. Bartram, Inorg. Chem. 5 (1966) 749.
[6] M. Tang, K.S. Holliday, J.A. Valdez, B.P. Uberuaga, P.O. Dickerson, R.M. Dickerson, Y. Wang, K.R. Czerwinski, K.E. Sickafus, J. Nucl. Mater. 389 (2009) 497.
[7] A. Guinier, X-Ray Diffraction in Crystals, Imperfect Crystals and Amorphous Bodies, Dover Publications, Inc., New York, 1994.
[8] H. Dosch, Phys. Rev. B 35 (1987) 2137.
[9] D. Simeone, J.L. Bechade, D. Gosset, A. Chevarier, P. Daniel, H. Pilliaire, G. Baldinozzi, J. Nucl. Mater. 281 (2000) 171.
[10] J.F. Ziegler, J.P. Biersack, U. Littmark, The Stopping and Range of Ions in Solids, Pergamon Press, New York, 1985.
[11] International Centre for Diffraction Data, Powder Diffraction File, Joint Committee on Powder Diffraction Standards, Philadelphia, PA, 1974–present.
[12] K.E. Sickafus, R.W. Grimes, J.A. Valdez, A. Cleave, M. Tang, M. Ishimaru, S.M. Corish, C.R. Stanek, B.P. Uberuaga, Nat. Mater. 6 (2007) 217.
[13] J.A. Valdez, M. Tang, K.E. Sickafus, Nucl. Instr. Meth. B 250 (2006) 148.
[14] M. Ishimaru, Y. Hirotsu, M. Tang, J.A. Valdez, K.E. Sickafus, J. Appl. Phys. 102 (2007) 063532.
[15] J. Lian, J. Chen, L.M. Wang, R.C. Ewing, J. Matt Farmer, L.A. Boatner, K.B. Helean, Phys. Rev. B 68 (2003) 134107.
[16] R.C. Ewing, W.J. Weber, J. Lian, J. Appl. Phys. 95 (2004) 5949.
[17] K.E. Sickafus, L. Minervini, R.W. Grimes, J.A. Valdez, M. Ishimaru, F. Li, K.J. McClellan, T. Hartmann, Science 289 (2000) 748.